Mapping Rice Planted Area Using a New Normalized EVI and SAVI (NVI) Derived From Landsat-8 OLI

Peng Li, Chiwei Xiao, and Zhiming Feng

***Abstract*— Obtaining annually updated data of actually planted rice paddy is essential for evaluating food security and estimating methane emission. Paddy field in southern China generally displays unique phenological landscape changes from exposed soils, shallow flooding water, to rice plants during the whole growth period in a year. A phenology-based algorithm was developed to map the rice planted paddies in the Poyang Lake Plain (PLP), China, in 2014, a typical region in Central China single- and double-rice cropping belt. This algorithm, or a normalized vegetation index, was based on the normalization of Landsat-8 Operational Land Imager-derived enhanced vegetation index and soil-adjusted vegetation index. It highlighted the temporal differences in vegetation cover and background soil between two critical growth phases of paddy rice, i.e., the flooding to transplanting stage and reproductive to ripening stage. There was estimated to be 7148.31 km^2 in the PLP, with an overall accuracy of 96.8% and the kappa coefficient of 0.97. Comparison between Landsat-detected results and the statistics of paddy field at the county level showed a high determination coefficient with the R^2 of 0.88. The phenology-based algorithm greatly facilitates rice farming monitoring at the regional scale.**

***Index Terms*— Enhanced vegetation index (EVI), Landsat, rice planted paddy, soil-adjusted vegetation index (SAVI).**

I. Introduction

UPDATED information of rice-planted area is indispensable for delineating rice cropping systems [1], [2] and monitoring methane emission [3]. Often, annual stock data of paddy fields is frequently used but neglecting the interannual variations due to farmland occupation, abandonment, and transformation [4]. It thus makes developing new and robust algorithms to obtain timely information of rice-cultivated area an important issue. Remote sensing of rice-planted paddies in tropical and subtropical regions are often complex owing to weather condition (e.g., cloud cover and its shadows) and multiple cropping systems [5], hence always gaining continuous attention [6], [7]. The major problems of these methods originate from two aspects, namely, spectral and radiometric settings of satellite sensors and weather condition. Currently, optical data is either featured by short revisit period but coarse spatial resolution, e.g., Moderate Resolution Imaging Spectroradiometer (MODIS [8]) or long revisit period but fine spatial resolution, such as Landsat. Meanwhile, synthetic aperture radar data can also be used to extract rice-planted area and sometimes outperform optical sensor imagery [9]. However, it also leads to misclassification due to similar backscattering values [6] or prone-suffered speckles [8]. Also, the high cost of imagery access is another hindrance for extensive studies.

A unique physical feature of paddy fields is the seasonal land cover changes from exposed soils (sometimes with weeds), shallow flooding water (a depth of 3–5 cm), to rice plants annually [1], [2]. Correspondingly, the temporal development of rice fields can be categorized into three main periods: 1) the fallow period after harvest and before sowing next year (Period A); 2) the flooding and rice seedlings transplanting period (Period B); and 3) the rice growing period (Period C) [9]. Vegetation indices (VIs) are recognized as robust indicators for monitoring temporal dynamics of rice farming, especially in the Period B (over two weeks) [10]. There exists a temporal anomaly between the normalized difference VI (NDVI) or enhanced VI (EVI) [11] and land surface water index (LSWI) during the Period B [12]. Afterward, the phenology-based paddy rice mapping algorithm based on the relationship of these VIs was first applied in large-scale regions with MODIS images, such as southern China [13] and South and Southeast Asia [7]. Since then, scientists have utilized this unique feature of paddy rice for mapping paddy field in global rice producing area with single-, double-, and triple-rice cropping systems [14]–[16]. However, the mixed-pixel problem was always questioned due to frustrating lower classification accuracy at county to regional scale.

In comparison, Landsat Thematic Mapper (TM), Enhanced TM Plus, and Operational Land Imager (OLI) 30-m spatial resolution data might significantly overcome the mixed pixel issue [1], [2], [14], especially because of the free availability policy [17]. Before 2008, the limited access because of high cost of Landsat data was one of the major reasons for its underutilization [18], particularly in the aspects of developing phenology-based algorithms to monitor paddy rice and its cropping intensity. Because the anomaly of Landsat-derived NDVI (or EVI) and LSWI is less obvious during the flooding

Manuscript received April 3, 2018; revised May 24, 2018 and July 11, 2018; accepted July 15, 2018. Date of publication September 3, 2018; date of current version December 5, 2018. This work was supported in part by the Opening Fund of Key Laboratory of Poyang Lake Wetland and Watershed Research (Jiangxi Normal University), Ministry of Education of China under Grant PK2016004 and in part by the National Natural Science Foundation of China under Grant 41430861. *(Corresponding author: Zhiming Feng.)*

The authors are with the Institute of Geographic Sciences and Natural Resources Research, Chinese Academy of Sciences, Beijing 100101, China, and also with the University of Chinese Academy of Sciences, Beijing 100049, China (e-mail: lip@igsnrr.ac.cn; xiaocw@igsnrr.ac.cn; fengzm@igsnrr.ac.cn).

Color versions of one or more of the figures in this letter are available online at http://ieeexplore.ieee.org.

Digital Object Identifier 10.1109/LGRS.2018.2865516

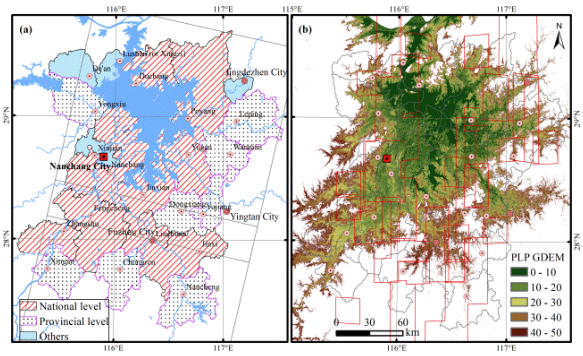

Fig. 1. Maps of the study area in Jiangxi Province, China, showing (a) PLP defined by the elevation less than or equal to (b) 50 m with Advanced Spaceborne Thermal Emission and Reflection Radiometer Global Digital Elevation Model. The red polygons in (b) represent the footprints of finer resolution images provided by GE for results validation.

and transplanting period (Period B) of paddy rice in the Poyang Lake Plain (PLP), in Central China single- and double-cropping rice cultivated regions, new combinations of VIs need to be explored and validated.

In this letter, a simple and novel algorithm, or the normalized VI (NVI), via the normalization of OLI-derived EVI and soil-adjusted VI (SAVI) [19] which considerably reduces the saturation effects [11], was developed to detect and map the rice-planted paddy in 2014. The objective was to assess the potential of the OLI-derived NVI in effectively mapping rice-planted area at the pixel level. If feasible, it will contribute to reconstructing historical data of actually cultivated paddy fields, rather than relying on local disputed statistics.

II. Materials and Methods

A. Study Area

The PLP, or the typographically flat area with an elevation below 50 m around China's largest freshwater lake [Fig. 1(b)], is an important part of middle-lower Yangtze Plain and Central China single- and double-cropping rice cultivated regions. There are two rice cropping systems, namely, the single-cropping system (SCS) and double-cropping system (DCS), which consist of three rice seasons (early, single, and late rice). Paddy fields of SCS and DCS are spatially independent, which indicates the summation of both equals to the total rice-planted area each year. With regard to local phenology of paddy rice, it has been clearly clarified in [1] and [2].

With the predominant biophysical conditions, the PLP, including 25 county-level administrative units [Fig. 1(a)], is home to many provincial and national level major rice-producing counties or cities in northern Jiangxi Province. However, the traditional rice production and provisioning function has been transformed into supplies of other more profitable cash crops (e.g., fruits, vegetables, and cotton) in the last decades. In addition, increasing farmland abandonment due to labor forces flowing into urban areas and occupied by urbanization also undermine the status of rice producing base.

B. Landsat-8 OLI Data Products

Landsat products were freely gathered from the U.S. Geological Survey Earth Resources Observation and Science Center Science Processing Architecture on Demand Interface.

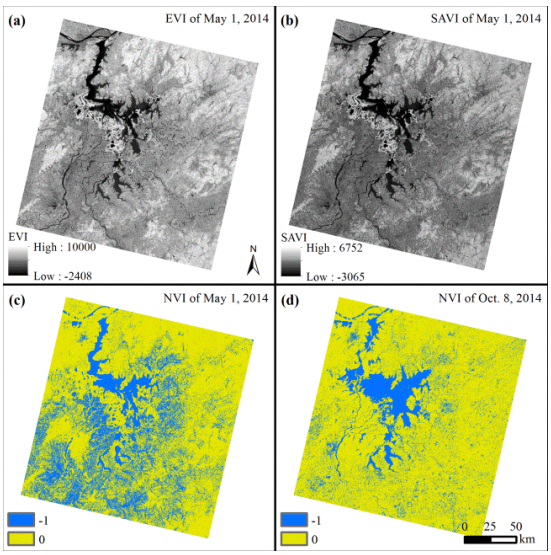

Fig. 2. Maps of (a) Landsat OLI-derived EVI, (b) SAVI, and (c) and (d) NVIs of one footprint (path/row: 121/040) covering the major part of the PLP of China on May 1, 2014 and October 8, 2014.

The products include the surface reflectance of multispectral bands, C version Function of Mask (CFmask) data, and several spectral indices [e.g., NDVI, EVI, and SAVI, see (1)–(3)]. These level-1 terrain corrected data have been consistently carried out radiometric, geometric, and precision correction, and also parallax error correction with digital elevation model because of local topographic relief. According to the local phenological calendar of paddy rice [1], [2], both EVI and SAVI derived from two pairs of OLI scenes (path/row: 121/040 and 121/041) acquired on May 1, 2014 [Fig. 2(a) and (b)] and October 8, 2014 were used to establish the normalized algorithm of NVI for detecting rice-planted paddy. The scene of October 8 and another scene acquired on August 5 were used to identify rice cropping systems with the resultant map of rice paddy in 2014. All the contaminated pixels of cloud and cloud shadow were excluded by means of the CFmask data for further analysis.

$$\mathrm{NDVI} = \frac{\rho_{\mathrm{NIR}} - \rho_{\mathrm{red}}}{\rho_{\mathrm{NIR}} + \rho_{\mathrm{red}}} \tag{1}$$

$$\mathrm{EVI} = 2.5 * \frac{\rho_{\mathrm{NIR}} - \rho_{\mathrm{red}}}{\rho_{\mathrm{NIR}} + 6 * \rho_{\mathrm{red}} - 7.5 * \rho_{\mathrm{blue}} + 1} \tag{2}$$

$$\mathrm{SAVI} = \frac{\rho_{\mathrm{NIR}} - \rho_{\mathrm{red}}}{\rho_{\mathrm{NIR}} + \rho_{\mathrm{red}} + L} * (1 + L) \tag{3}$$

where ρ_{NIR}, ρ_{red}, and ρ_{blue} refer to the surface reflectance of near infrared (NIR), red, and blue bands of Landsat OLI sensor, respectively. The parameter of L in the equation of SAVI represents the soil brightness correction factor, and its value ranging from 0 to 1 varies according to the change of vegetation cover. For very high vegetation regions, L is assigned as zero, effectively turning SAVI into NDVI. Typically, the default value ($L = 0.5$) is used for most situations, especially when vegetation cover is unknown.

C. Algorithms for Mapping Rice-Planted Paddies and Rice Cropping Systems

The Landsat-based NVI (4) represents the normalization of EVI and SAVI established using the principle similar to the

NDVI equation. The NVI was applied to highlight the temporal differences from water content to vegetation cover of paddy rice from flooding and rice transplanting stage (Period B) to growth stage (including reproductive and ripening stages, Period C).

$$\mathrm{NVI} = \frac{\mathrm{EVI} - \mathrm{SAVI}}{\mathrm{EVI} + \mathrm{SAVI}}. \tag{4}$$

Using the NVI algorithm to detect rice-planted paddies was comprised of two key steps. One is the NVIs calculation with a single-date image (May 1, 2014 or October 8, 2014) during the two periods, i.e., Period B and Period C. The results showed that the NVI values of water-related pixels were consistently equal to -1, while the others typically amount to zero [Fig. 2(c) and (d)]. It can be inferred that the NVI shows high sensitivity to water content either in Period B or Period C. For paddy rice farming, the rice-planted paddies generally need a necessary duration of flooding for rice seedlings transplantation and turning green or reviving after root injuries. During the whole growth period from late March to late October, only paddy fields experience landscape changes from shallow water surface (also mixed with exposed soils and sparse rice seedlings) to well-grown rice plants *in situ*. The second step is to extract the target pixels with values changed from negative 1 to zero, between two critical temporal windows or from May 1 to October 8. Also, a water mask derived from the image of October 8 was further used to avoid the potential effects of permanent shallow water on the final determination of rice-planted area.

With the resultant map of rice-planted paddies, the SCS and DCS were discriminated with the scenes of August 5, 2014 and October 8, 2014 using the renormalized index of NDVI (RNDVI) approach [1].

$$\mathrm{RNDVI} = (|\mathrm{NDVI}_{t1}| - |\mathrm{NDVI}_{t2}|)/(|\mathrm{NDVI}_{t1}| + |\mathrm{NDVI}_{t2}|) \tag{5}$$

where $t1$ and $t2$ refer to the acquisition dates of two Landsat scenes (e.g., August 5, 2014 and October 8, 2014) and, NDVI_{t1} and NDVI_{t2} are the corresponding NDVIs showing inverse change for two rice cropping systems, SCS and DCS.

D. Validation and Comparison

Field geo-tagged photographs of paddy rice were corrected in 39 villages/towns of seven major rice-producing counties (including Nanchang, Xinjian, Jinxian, Yugan, Poyang, Wannian, and Yongxiu) in the PLP during August 13, 2014–August 19, 2014. In addition, more photographs were gathered in other field trips of rice cropping systems in 2007, 2008, 2010–2012, and 2015, respectively. These photographs were necessary for understanding the imaging characteristics of paddy field and other land cover types based on finer spatial resolution imagery (a total of 27 polygons) provided by Google Earth (GE) [Fig. 1(b)]. In this letter, the photographs gathered in 2014 were exclusively applied to generate the region of interests (ROIs) for rice-planted paddy and nonpaddy field. Accuracy assessment of the resultant map of rice-planted paddies was performed using the confusion matrix. The random reference data samples consisted of 41 916 pixels extracted from 215 ROIs for rice-planted paddy and 21 334 pixels from 207 ROIs for the nonpaddy types of land cover.

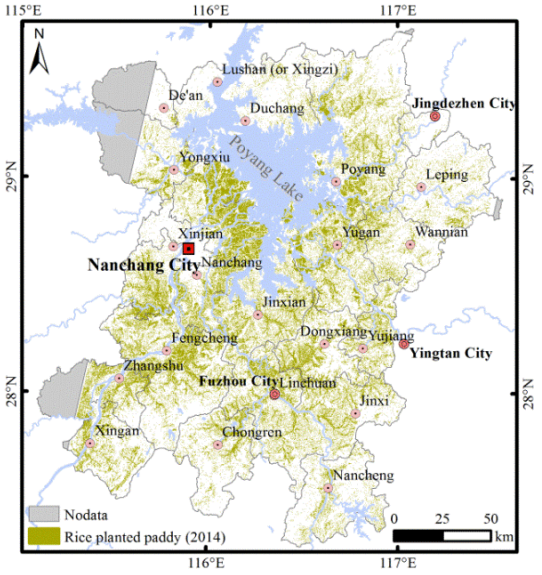

Fig. 3. Map of the NVI-derived rice-planted paddy in the PLP, China, in 2014.

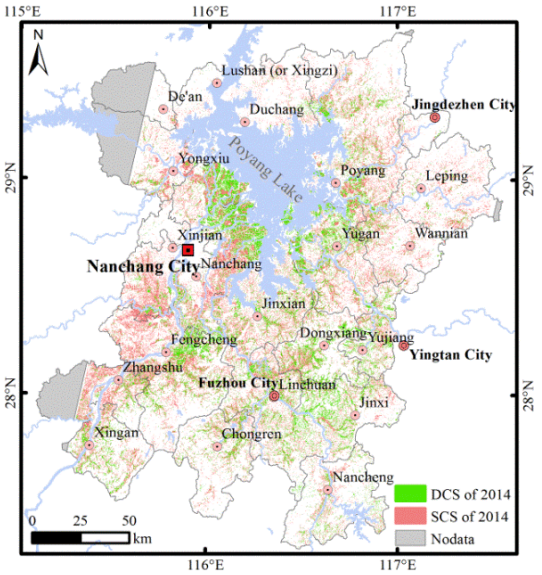

Fig. 4. Map of the RNDVI derived rice cropping systems in the PLP, China, in 2014.

III. Mapping Rice-Planted Paddies Using the NVI Algorithm in 2014

Fig. 3 showed the distribution of the actually planted rice paddy in the PLP in 2014 based on the normalization algorithm of OLI-derived EVI and SAVI (or the NVI) between May 1, 2014 and October 8, 2014. There was an estimated 7148.31 km^2 in the major rice-producing area of the PLP. Fig. 4 further showed the area of SCS and DCS estimated with the scenes of August 5, 2014 and October 8, 2014 with the RNDVI method. The areas of the SCS and DCS were 4493.17 and 2655.14 km^2, respectively. The multiple cropping indexes at the county level ranged from 112% in Lushan City (county level) of Jiujiang city to 153% in Jinxi County of

TABLE I

ACCURACY ASSESSMENT OF LANDSAT-DERIVED RESULTANT MAP OF RICE-PLANTED AREA BASED ON THE NORMALIZATION OF EVI AND SAVI (NVI)

Class		Google Earth selected samples (pixels)		Total classified pixels	Producer accuracy
		Rice paddy	Non rice paddy		
Classified results	Rice paddy	40532	1384	41916	98.5%
	Non rice paddy	610	20724	21334	93.7%
Total ground truth (pixels)		41142	22108	63250	
User accuracy		96.7%	97.1%		

Overall accuracy is 96.8%; Kappa coefficient is 0.97.

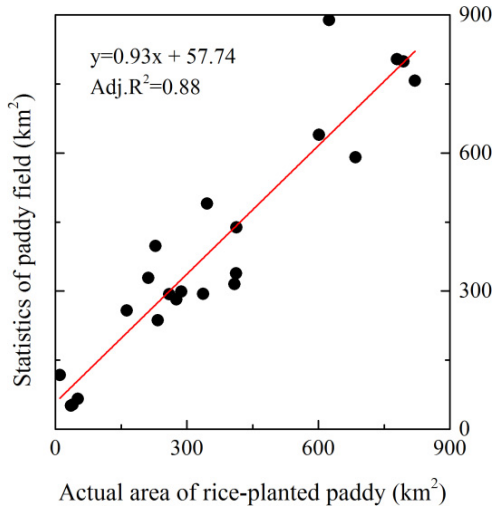

Fig. 5. Linear relationship between the resultant rice-planted paddies derived with the normalization of Landsat EVI and SAVI (or the NVI) and the paddy field statistics at the county level in the PLP in 2014.

Fuzhou city. Spatially, rice-planted paddies were intensively distributed in the fluvial–alluvial plain of the four major rivers (i.e., Ganjiang, Fuhe, Xinjiang, and Raohe) in Jiangxi Province.

The resultant map of rice-planted paddy is highly accurate according to the confusion matrix estimated from random reference data samples (Table I). The producer's accuracies in mapping rice-planted paddies and nonpaddy land cover were 93.7% and 98.5%, respectively, while the user accuracies equal to 96.7% and 97.1%, respectively. The overall accuracy of the resultant map was 96.8% with the Kappa coefficient up to 0.97. In addition, there was a linear relationship between the NVI-derived data of rice paddy and the paddy field statistics at the county level (Fig. 5), with the R^2 value of 0.88. Data from De'an County, Yongxiu County, and Zhangshu city were not accounted because of the missing data.

IV. CONCLUSION AND DISCUSSION

A novel and effective phenology-based algorithm was developed to detect and map the actually rice-planted paddies in 2014 through the normalization of Landsat-8 OLI derived EVI and SAVI (or the NVI) in the PLP, a typical region of Central China single and double cropping rice cultivated systems. The algorithm based on the unique physical feature of paddy fields, highlighted the seasonal landscape changes among exposed soils, shallow water cover, and growing rice plants. The rice-producing area of the PLP was 7148.31 km^2 in 2014. The NVI is not only suitable for extracting the vast continuous paddy fields in the river alluvium plains but also fits to identify the terraced fields distributed in arborescent type in the hilly area and downlands. The accuracy of rice-planted paddies detection was satisfying with high overall accuracy and Kappa coefficient. It clearly indicates that the phenology-based algorithms (NVI and RNDVI) hold great potential in mapping rice-planted paddies and cropping intensity.

With the combination of the NVI and the RNDVI algorithms [1], it well figures out an everlasting question about how to monitor the actually planted rice paddies and rice cropping systems (or planting intensity) using Landsat images acquired during the rice growth period in the same year. The algorithms established via the combined usage of Landsat-derived VIs greatly reduce the demand of satellites data. Only two pairs of Landsat images fully meet the data requirements for timely detecting annual information of rice paddy. In addition, both algorithms were developed with visible (red and blue) and NIR bands only, which enhance their applicability with data of other Landsat-like sensors. The physical basis of the RNDVI is the phenological differences among early-, single- and late rice, or between the SCS and DCS in Central China single- and double-cropping rice cultivated region with a tight phenological arrangement. The usage of dual-time windows fully observes the phenological features of rice growth, which ensures the method's objectivity and avoids the subjectivity handled in a single-date way. However, the innovation of spectral VIs normalization may have limitation for its suitability in the regions with loose phenological arrangement, particularly in the tropical rice-producing regions, e.g., the Mekong delta in Southeast Asia.

REFERENCES

[1] P. Li, L. Jiang, Z. Feng, S. Sheldon, and X. Xiao, "Mapping Rice cropping systems using Landsat-derived Renormalized Index of Normalized Difference Vegetation Index (RNDVI) in the Poyang Lake Region, China," *Frontiers Earth Sci.*, vol. 10, no. 2, pp. 303–314, 2016.

[2] P. Li, Z. Feng, L. Jiang, Y. Liu, and X. Xiao, "Changes in Rice cropping systems in the Poyang Lake Region, China during 2004–2010," *J. Geograph. Sci.*, vol. 22, no. 4, pp. 653–668, 2012.

[3] S. Weller *et al.*, "Greenhouse gas emissions and global warming potential of traditional and diversified tropical Rice rotation systems," *Global Change Biol.*, vol. 22, no. 1, pp. 432–448, 2016.

[4] E. Lichtenberg and C. Ding, "Assessing farmland protection policy in China," *Land Use Policy*, vol. 25, no. 1, pp. 59–68, 2008.

[5] K.-R. Manjunath, R.-S. More, N.-K. Jain, S. Panigrahy, and J.-S. Parihar, "Mapping of Rice-cropping pattern and cultural type using remote-sensing and ancillary data: A case study for South and Southeast Asian countries," *Int. J. Remote Sens.*, vol. 36, no. 24, pp. 6008–6030, 2015.

[6] K. Okamoto and H. Kawashima, "Estimation of Rice-planted area in the tropical zone using a combination of optical and microwave satellite sensor data," *Int. J. Remote Sens.*, vol. 20, no. 5, pp. 1045–1048, 1999.

[7] X. Xiao *et al.*, "Mapping paddy Rice agriculture in South and Southeast Asia using multi-temporal MODIS images," *Remote Sens. Environ.*, vol. 100, no. 1, pp. 95–113, 2006.

[8] M.-K. Mosleh, Q.-K. Hassan, and E.-H. Chowdhury, "Application of remote sensors in mapping Rice area and forecasting its production: A review," *Sensors*, vol. 15, no. 1, pp. 769–791, 2015.

[9] T. L. Toan *et al.*, "Rice crop mapping and monitoring using ERS-1 data based on experiment and modeling results," *IEEE Trans. Geosci. Remote Sens.*, vol. 35, no. 1, pp. 41–56, Jan. 1997.

[10] C. Kontgis, A. Schneider, and M. Ozdogan, "Mapping Rice paddy extent and intensification in the Vietnamese Mekong River Delta with dense time stacks of Landsat data," *Remote Sens. Environ.*, vol. 169, pp. 255–269, Nov. 2015.

[11] A.-R. Huete, H.-Q. Liu, K. Batchily, and W. J. D. A. Van Leeuwen, "A comparison of vegetation indices over a global set of TM images for EOS-MODIS," *Remote Sens. Environ.*, vol. 59, no. 3, pp. 440–451, 1997.

[12] X. Xiao *et al.*, "Observation of flooding and Rice transplanting of paddy Rice fields at the site to landscape scales in China using VEGETATION sensor data," *Int. J. Remote Sens.*, vol. 23, no. 15, pp. 3009–3022, 2002.

[13] X. Xiao *et al.*, "Mapping paddy Rice agriculture in southern China using multi-temporal MODIS images," *Remote Sens. Environ.*, vol. 95, no. 4, pp. 480–492, 2005.

[14] J. Dong *et al.*, "Mapping paddy Rice planting area in northeastern Asia with Landsat 8 images, phenology-based algorithm and Google Earth Engine," *Remote Sens. Environ.*, vol. 185, pp. 142–154, Nov. 2016.

[15] D. Peng, A.-R. Huete, J. Huang, F. Wang, and H. Sun, "Detection and estimation of mixed paddy Rice cropping patterns with MODIS data," *Int. J. Appl Earth Observ. Geoinf.*, vol. 13, no. 1, pp. 13–23, 2011.

[16] T. Sakamoto, C. van Phung, A. Kotera, K.-D. Nguyen, and M. Yokozawa, "Analysis of rapid expansion of inland aquaculture and triple Rice-cropping areas in a coastal area of the Vietnamese Mekong Delta using MODIS time-series imagery," *Landscape Urban Planning*, vol. 92, no. 1, pp. 34–46, 2009.

[17] C.-E. Woodcock *et al.*, "Free access to Landsat imagery," *Science*, vol. 320, no. 5879, pp. 1011–1012, 2008.

[18] J.-A. Martinez-Casasnovas, A. Martín-Montero, and M.-A. Casterad, "Mapping multi-year cropping patterns in small irrigation districts from time-series analysis of Landsat TM images," *Eur. J. Agron.*, vol. 23, no. 2, pp. 159–169, 2005.

[19] A.-R. Huete, "A soil-adjusted vegetation index (SAVI)," *Remote Sens. Environ.*, vol. 25, no. 3, pp. 295–309, 1988.